10-1-1993

Fluttering fountains: Simplified models

Lee W. Casperson
Portland State University

Citation Details

Casperson, L. W. (1993). Fluttering fountains: Simplified models. Journal Of Applied Physics, 74(8), 4894.

Fluttering fountains: Simplified models

Lee W. Casperson
Department of Electrical Engineering, Portland State University, P. O. Box 751, Portland, Oregon 97207-0751

(Received 12 April 1993; accepted for publication 15 June 1993)

Fluttering oscillations are sometimes observed in the falling sheets of water associated with dams and waterfall fountains, and a theoretical simulation of this phenomenon was recently reported. In this study approximate analytical solutions of the previous model are described and compared with the experimental and theoretical observations.

I. INTRODUCTION

Fluttering oscillations have been observed in the thin sheets of water associated with some dams since the early 1800s,[1] and they continue to be reported up to the present.[2] Similar oscillations are sometimes seen in waterfall fountains, and a detailed review and theoretical simulation of this phenomenon were recently reported.[3] The underlying instability is related to the shear flow instability of surfaces separating fluids moving at different velocities, as first discussed by Helmholtz.[4] More common examples of the Helmholtz instability mechanism are the generation of water waves by wind, or the flapping of a flag. In the case of the fluttering fountain instability a sheet of water is moving through the surrounding air, and it is not necessary that there be any wind or overall motion of the air.

The fluttering fountain oscillations differ from wind-generated water waves in that the fountain oscillations may be extremely periodic, while most other water waves are typically irregular. Periodic behavior always suggests the existence of a feedback mechanism, and the feedback in this case is provided by the confined air chamber behind the water sheet. The large-amplitude wave motions at the bottom of the sheet tend to compress or expand the trapped air, which in turn pulls in or pushes out on the water surface at the top. The small displacements at the top are amplified by the Helmholtz mechanism as the sheet falls, and thus the oscillations are maintained.

Two different oscillation modes of a typical waterfall fountain are shown in Fig. 1. This particular fountain is one of two large systems located in Dunedin, New Zealand, in the Octagon, the city's central park. The author had the opportunity to study the behavior of these fountains during a recent sabbatical leave at the University of Otago in Dunedin.[3] We were able to vary the flow rate, and by adjusting the depth of the water in the lower pool the effective height of the fountain was also adjustable. For large heights and low flow rates, the water sheet exhibited noisy and usually periodic oscillations. For lower heights and larger flow rates the water sheet was stable. Many features of these oscillations were found to be in agreement with the numerical solutions of a theoretical model. These numerical solutions are somewhat complicated, and in the present study we explore some of the simpler analytical solutions implied by the same model.

The theoretical model for the fluttering fountain instability is briefly summarized in Sec. II, and a systematic simplification of the model is undertaken. Specific results include approximate analytical forms for the wave shape and the gain, and examples of these results are given in Sec. III. The analytical results are also compared with experimental data from the Dunedin fountains.

II. THEORY

For purposes of analysis, the fluttering fountains have been idealized to a nearly vertical water sheet flowing across a rectangular chamber, which represents the air confined behind the water. This simplified arrangement and the corresponding coordinate system are sketched in Fig. 2. The water becomes free of the weir and subject to air currents in front and back starting at the height y_0 with downward velocity v_0. The air chamber has a horizontal depth x_0.

A rigorous understanding of this fluid instability requires an appropriate set of governing differential equations. The equations developed in our previous study include the set[3]

$$\frac{\partial u(y,t)}{\partial t}=\left(\frac{1}{\rho_w F}\left\{\Delta p_f(t)+\rho_a\omega v(y)\left[\coth\left(\frac{\omega x_0}{v(y)}\right)+\left(1+\frac{v_a}{v(y)}\right)^2\right]D(y,t)\right\}+\frac{\partial u(y,t)}{\partial y}\right)v(y), \tag{1}$$

$$\frac{\partial D(y,t)}{\partial t}=u(y,t)+v(y)\frac{\partial D(y,t)}{\partial y}, \tag{2}$$

$$\frac{d\Delta p_f(t)}{dt}=-\gamma\frac{P_0+\Delta p_f(t)}{A+\int_0^{y_0}D(y,t)dy}\int_0^{y_0}\frac{\partial D(y,t)}{\partial t}dy, \tag{3}$$

where $u(y,t)$ is the time- and height-dependent x component of the velocity, $D(y,t)$ is the displacement in the x direction, and $\Delta p_f(t)$ is the time-dependent pressure difference across the sheet due to possible compression or expansion of the air in the chamber behind the water. The downward velocity of the water sheet is represented by $v(y)$, which can be written approximately

$$v(y)=v_0[1-2g(y-y_0)/v_0^2]^{1/2}. \tag{4}$$

The other constants appearing in these equations include the air density ρ_a, the water density ρ_w, the flow rate in cubic meters per meter of weir length per second F, the radian frequency of the oscillations ω, the effective depth of the air chamber behind the water sheet x_0, and the upward

 0021-8979/93/74(8)/4894/5/$6.00

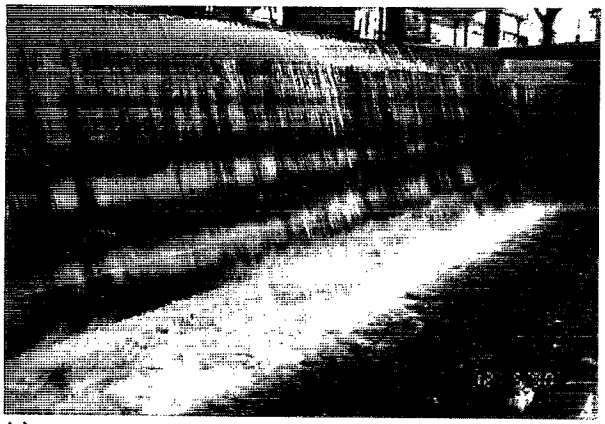

(a)

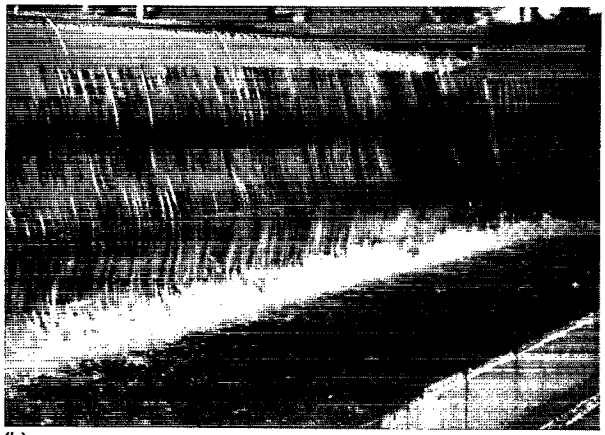

(b)

FIG. 1. Two typical periodic oscillation modes of the No. 1 waterfall fountain in Dunedin, New Zealand.

velocity of any wind against the waterfall v_a. The downward velocity of the water as it separates from the weir is v_0, the acceleration of gravity is 9.8 m/s^2, the specific heat ratio for the air is $\gamma=1.4$, the background atmospheric pressure is P_0, the height of the fall is y_0, and $A=x_0y_0$ is the cross-sectional area of the air chamber in the absence of oscillations.

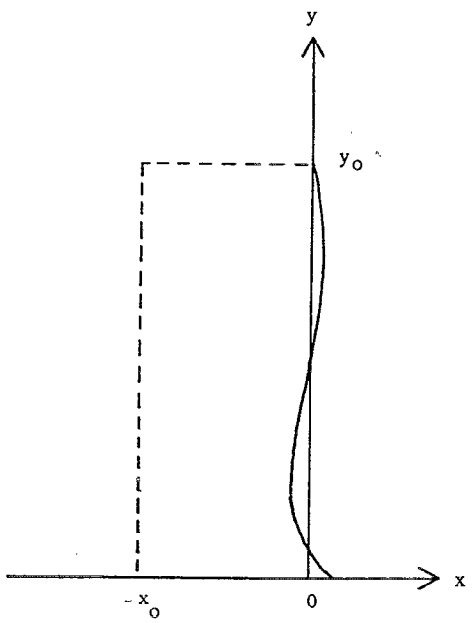

FIG. 2. Simplified fountain configuration for numerical and analytical computations.

Equations (1)–(4) form a complete set from which the velocities, displacements, and pressures can all be obtained. These equations are actually somewhat more complicated than they may appear, because Eqs. (1) and (2) must be solved for each of the height segments into which the falling water is divided. We have found that to obtain reasonable accuracy 20 or more height steps are required. Thus it would be helpful in studying these systems if some progress toward analytic solutions were possible.

As a first step toward solving Eqs. (1)–(4), it may be noted that in Eqs. (1)–(3) are almost linear in the variables $u(y,t)$, $D(y,t)$, and $\Delta p_f(t)$. In fact these equations become linear if one drops the term $\Delta p_f(t)$ in the numerator of Eq. (3) and the integral of $D(y,t)$ in the denominator. We have verified by means of numerical solutions that these terms have no significant effect on the solution of Eqs. (1)–(4). Thus we now replace Eq. (3) by the linear result

$$\frac{d\Delta p_f(t)}{dt}=-\frac{\gamma P_0}{A}\int_0^{y_0}\frac{\partial D(y,t)}{\partial t}\,dy. \tag{5}$$

With the simpler linear form of the equations one is led to look for a sinusoidal time dependence of the dependent variables. Our numerical solutions indicate that the time dependencies are essentially indistinguishable from sinusoidal variations, and this conclusion is also in agreement with many of our experimental observations. Thus it is reasonable to write the dependent variables in the forms

$$u(y,t)=\mathrm{Re}\,u'(y)\exp(i\omega t), \tag{6}$$

$$D(y,t)=\mathrm{Re}\,D'(y)\exp(i\omega t), \tag{7}$$

$$\Delta p_f(t)=\mathrm{Re}\,\Delta p'_f\exp(i\omega t). \tag{8}$$

With these substitutions, Eqs. (1), (2), and (5) can be written

$$\frac{du'(y)}{dy}=i\frac{\omega}{v(y)}u'(y)-\frac{1}{\rho_w F}\left\{\Delta p'_f+\rho_a\omega v(y)\times\left[\coth\left(\frac{\omega x_0}{v(y)}\right)+\left(1+\frac{v_a}{v(y)}\right)^2\right]D'(y)\right\}, \tag{9}$$

$$\frac{dD'(y)}{dy}=i\frac{\omega}{v(y)}D'(y)-\frac{1}{v(y)}u'(y), \tag{10}$$

$$\Delta p'_f=-\frac{\gamma P_0}{A}\int_0^{y_0}D'(y)dy. \tag{11}$$

Equations (9)–(11) are simpler than Eqs. (1), (2), and (5) in the sense that the time dependence has now been eliminated. However, the new set still includes integro-differential equations, and the solutions are not simple. We have obtained solutions of these equations by

an iterative integration method and verified that the results are consistent with our numerical solutions of the previous set.

A further simplification is obtained if the complex velocity and displacement variables are expanded according to

$$u'(y)=u''(y)\exp[-i\omega v(y)/g], \tag{12}$$

$$D'(y)=D''(y)\exp[-i\omega v(y)/g]. \tag{13}$$

With these substitutions, Eqs. (9) and (10) reduce to

$$\frac{du''(y)}{dy}=-\frac{\Delta p'_f}{\rho_w F}\exp\left(\frac{i\omega v(y)}{g}\right)-\frac{\rho_a\omega v(y)}{\rho_w F}\times\left[\coth\left(\frac{\omega x_0}{v(y)}\right)+\left(1+\frac{v_a}{v(y)}\right)^2\right]D''(y), \tag{14}$$

$$\frac{dD''(y)}{dy}=-\frac{1}{v(y)}u''(y), \tag{15}$$

where we have also used the relationship[3]

$$\frac{1}{v(y)}=-\frac{d}{dy}\left(\frac{v(y)}{g}\right). \tag{16}$$

Thus, this variable change leads to the elimination of two terms from the governing equations.

It is also helpful to use the velocity v as the independent variable, and then Eqs. (14) and (15) become

$$\frac{du''(v)}{dv}=\frac{v\Delta p'_f}{g\rho_w F}\exp\left(\frac{i\omega v}{g}\right)+\frac{\rho_a\omega v^2}{g\rho_w F}\times\left[\coth\left(\frac{\omega x_0}{v}\right)+\left(1+\frac{v_a}{v}\right)^2\right]D''(v), \tag{17}$$

$$\frac{dD''(v)}{dv}=\frac{1}{g}u''(v). \tag{18}$$

Now the dependent variable u'' can be eliminated between these equations, and we obtain the single second-order equation

$$\frac{d^2D''(v)}{dv^2}=\frac{v\Delta p'_f}{g^2\rho_w F}\exp\left(\frac{i\omega v}{g}\right)+\frac{\rho_a\omega v^2}{g^2\rho_w F}\times\left[\coth\left(\frac{\omega x_0}{v}\right)+\left(1+\frac{v_a}{v}\right)^2\right]D''(v). \tag{19}$$

To make further progress toward analytical solutions some approximations are required. Our numerical solutions show that the feedback pressure variations are small compared to amplification pressures except at the top of the fall, where $D''(v)$ approaches zero. The displacements caused by the pressure fluctuations also tend to average to zero over an acoustical cycle. Thus it is reasonable to neglect the feedback pressure $\Delta p'_f$ when estimating the possible shapes of the growing waves, and we approximate Eq. (19) by the equation

$$\frac{d^2D''(v)}{dv^2}=\frac{\rho_a\omega v^2}{g^2\rho_w F}\left[\coth\left(\frac{\omega x_0}{v}\right)+\left(1+\frac{v_a}{v}\right)^2\right]D''(v). \tag{20}$$

Equation (20) is an approximate equation for the envelope of the downward growing waves of a fluttering fountain. It may be noted that with the neglect of the pressure feedback term, there is no longer any coupling between the real and imaginary parts of the displacement amplitude $D''(v)$. Therefore, $D''(v)$ may be taken to be a real variable governed by a single ordinary differential equation. More important, the wave nature of the descending water sheet is now fully captured in the simple analytic factors given above in Eqs. (6), (7), (12), and (13). With minor additional simplifications explicit analytic solutions can also be obtained for the wave envelope.

For the experimental operating conditions of the Dunedin fountains, the argument $\omega x_0/v$ of the coth function is generally larger than unity, and thus the coth term may be approximately replaced by unity. If no wind is blowing ($v_a=0$), Eq. (20) may be simplified to

$$\frac{d^2D''(v)}{dv^2}-\alpha^2v^2D''(v)=0, \tag{21}$$

where we have introduced the coefficient α,

$$\alpha=\left(\frac{2\rho_a\omega}{g^2\rho_w F}\right)^{1/2}. \tag{22}$$

It is also helpful to introduce the new independent variable

$$x=(2\alpha)^{1/2}v. \tag{23}$$

With this substitution Eq. (21) reduces to

$$\frac{d^2D''(x)}{dx^2}-\frac{1}{4}x^2D''(v)=0. \tag{24}$$

Equation (24) may be recognized as an equation for the parabolic cylinder functions. One of the standard forms for such equations is[5]

$$\frac{d^2y}{dx^2}-\left(\frac{1}{4}x^2+a\right)y=0, \tag{25}$$

where the parameter y in this equation is, of course, unrelated to our height variable y. If a is set equal to zero, Eqs. (24) and (25) are equivalent. For large values of x and moderate values of a, the standard solutions of Eq. (25) can be expressed as the expansions[6]

$$U(a,x)\approx\exp\left(-\frac{x^2}{4}\right)x^{-a-1/2}\left(1-\frac{(a+\frac{1}{2})(a+\frac{3}{2})}{2x^2}+\frac{(a+\frac{1}{2})(a+\frac{3}{2})(a+\frac{5}{2})(a+\frac{7}{2})}{2(4x^4)}-\cdots\right), \tag{26}$$

$$V(a,x)\approx\left(\frac{2}{\pi}\right)^{1/2}\exp\left(\frac{x^2}{4}\right)x^{a-1/2}\left(1+\frac{(a-\frac{1}{2})(a-\frac{3}{2})}{2x^2}+\frac{(a-\frac{1}{2})(a-\frac{3}{2})(a-\frac{5}{2})(a-\frac{7}{2})}{2(4x^4)}+\cdots\right). \quad (27)$$

In our experiments the radian oscillation frequency was typically in the range $30<\omega<100\ \mathrm{s}^{-1}$.[3] Other typical parameters for use in Eq. (22) include $\rho_a=1.225\ \mathrm{kg\ m}^{-3}$, $\rho_w=10^3\ \mathrm{kg\ m}^{-3}$, $F=3\ \ell\mathrm{m}^{-1}\ \mathrm{s}^{-1}$, and $g=9.8\ \mathrm{m\ s}^{-2}$. With these substitutions one finds that the parameter α is typically on the order of $1\ \mathrm{s}^2\ \mathrm{m}^{-2}$. Since the velocity of the falling water is usually several meters per second, it follows from Eq. (23) that the parameter x is usually large compared to unity. From the leading terms in Eqs. (26) and (27), the displacement can be written approximately

$$D''(x)=A\frac{\exp(x^2/4)}{x^{1/2}}+B\frac{\exp(-x^2/4)}{x^{1/2}}, \quad (28)$$

where the coefficients A and B are integration constants that must be chosen to match any boundary conditions that one imposes.

Equation (28) may now be expressed in terms of velocity using Eq. (23), and the result is

$$D''(v)=A\frac{\exp(\alpha v^2/2)}{(2\alpha)^{1/4}v^{1/2}}+B\frac{\exp(-\alpha v^2/2)}{(2\alpha)^{1/4}v^{1/2}}. \quad (29)$$

Within the approximations already employed, it is reasonable to require that the displacement be zero at the top of the fall. With this constraint, Eq. (29) reduces to

$$D''(v)=\frac{C}{v^{1/2}}\sinh\left(\frac{\alpha}{2}(v^2-v_0^2)\right), \quad (30)$$

where C is a new amplitude coefficient. With Eqs. (7) and (13) the overall solution for the displacement as a function of velocity and time is now

$$D(v,t)=\frac{C}{v^{1/2}}\cos\left(\omega t-\omega\frac{v}{g}\right)\sinh\left(\frac{\alpha}{2}(v^2-v_0^2)\right). \quad (31)$$

The velocity is related to the height by Eq. (4), and thus the final formula for the displacement is

$$D(y,t)=\frac{C}{v_0^{1/2}[1+2g(y_0-y)/v_0^2]^{1/4}}\cos\left[\omega t-\omega\frac{v_0}{g}\times\left(1+\frac{2g(y_0-y)}{v_0^2}\right)^{1/2}\right]\sinh[\alpha g(y_0-y)]. \quad (32)$$

It follows from Eq. (32) that the fluttering fountain oscillations are in the form of downward propagating waves having amplitude and wavelength that increase as the waves descend. The amplitude coefficient C would depend on the details of the feedback and nonlinear saturation.[3] It may be seen from the last term in Eq. (32) that the amplitude gain of the falling sheet becomes almost exponential having the gain coefficient

$$\text{gain}=\alpha g=\left(\frac{2\rho_a\omega}{\rho_w F}\right)^{1/2}, \quad (33)$$

where the definition of α from Eq. (22) has been used.

The possible oscillation frequencies can also be estimated on the basis of Eq. (32). It follows from this equation that the total phase delay from the top of the waterfall to the bottom must be

$$\text{phase}=\frac{\omega v_0}{g}\left[\left(1+\frac{2gy_0}{v_0^2}\right)^{1/2}-1\right]. \quad (34)$$

It is reasonable to expect a 2π phase shift between adjacent oscillation modes, and thus the possible oscillation frequencies are given by

$$f=\frac{m+m_0}{(v_0/g)[(1+2gy_0/v_0^2)^{1/2}-1]}, \quad (35)$$

where m is an integer and m_0 measures the fundamental excess top-to-bottom phase shift necessary to assure the positive feedback for sustaining the oscillations. Equation (35), which has been obtained here from a simplified version of our numerical model, has also been given previously in a more qualitative discussion of the feedback conditions for an oscillating water sheet.[7] It has been argued that the parameter m_0 must always be approximately equal to $\frac{1}{4}$.[8] The corresponding phase shift of $\pi/2$ would tend to ensure that the transverse acceleration at the top of the sheet would be maximized when the transverse displacement at the bottom is maximized. As seen above, however, the actual dynamical equations are quite complex, and Eq. (35) is only obtained as a result of significant simplifications. The practical implications of these results are examined in the following section.

III. RESULTS

Using Eq. (35), the oscillation frequencies of a fluttering fountain can be estimated for any mode order. For the Dunedin fountains the appropriate parameter values are approximately $v_0=1.5\ \mathrm{m\ s}^{-1}$, $g=9.8\ \mathrm{m\ s}^{-2}$, $m_0=\frac{1}{4}$, and the integer m depends on the mode order of interest. With these values the frequency from Eq. (35) is plotted in Fig. 3 as a function of the fountain height. Also plotted in the figure is a set of experimental data points for conditions of $m=1$ periodic oscillations. Within the accuracy of this data, Eq. (35) provides a good representation of the experimental oscillation frequencies. For lower flow rates, such as those represented by the triangular data points in Fig. 3, the initial velocity is less than $1.5\ \mathrm{m\ s}^{-1}$. As a result, the experimental oscillation frequencies are slightly below the theoretical values given by the curves in the figure.

With the frequency data from Eq. (35), one can also plot the actual oscillation wave forms using Eq. (32). A set of these wave forms is given in Fig. 4 for a fountain of height $y_0=0.8$ m, flow rate $F=7.5\ 1\ \mathrm{m}^{-1}\ \mathrm{s}^{-1}$, and various values of the mode index m. The only adjustable parameter in these plots is the amplitude C. The waves with $m=5$ and 2 are seen to be in good agreement with the experimental wave forms shown in parts (a) and (b) of Fig. 1.

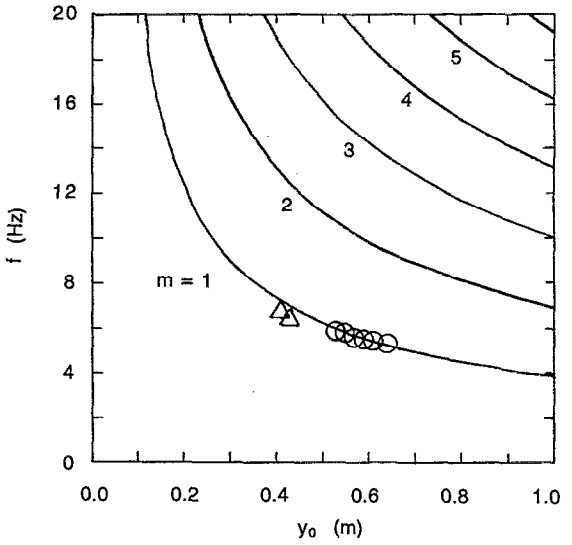

FIG. 3. Oscillation frequency as a function of fountain height for various values of the mode index m. Experimental data are for the No. 2 fountain at flow rates of 7.5 (circles) and 3 $\ell m^{-1} s^{-1}$ (triangles).

IV. DISCUSSION

The periodic oscillation modes of a fluttering fountain have been well described by a mathematical model which consists of a set of integro-differential equations. In this study we have explored a sequence of analytic simplifications of the model which lead ultimately to approximate closed-form solutions. These are found to retain the qualitative features of the theoretical oscillation behavior and to provide good agreement with many of the experimentally observed results. The resulting analytic formulas for the oscillation frequencies and wave forms are consistent with experimental data obtained with oscillating waterfall fountains located in Dunedin, New Zealand. The model can also be adapted to other fluid oscillator configurations.

While the fluttering fountains discussed here might seem to be quite different from other laboratory oscillators that one encounters, in fact their basic operating principles are common to many other systems. In particular, the fountains are simply an example of a general class of multimode feedback oscillators. In the fountains the necessary gain comes from the Helmholtz amplification of the falling waves, and the feedback from the bottom of the fountain to the top occurs through the confined air space behind the falling water sheet. As in all such oscillators the possible values of the round-trip delay are separated by an integer multiple of 2π, and the application of this oscillation phase condition leads to a set of mode frequencies that depend on the oscillator length. A well-known modern example of this type of oscillator is provided by lasers. In a laser the gain is usually provided by stimulated emission, and the feedback results from the mirrors which repeatedly direct the light signal back into the amplifying medium. In lasers the round-trip phase delay is also an integer multiple of 2π, and the length dependence of the mode frequencies is similar to the fountain results given in Fig. 3. Because electromagnetic waves travel about eight orders of magnitude faster than water waves, the laser mode frequencies are typically in the optical range while the fountain waves are infrasonic.

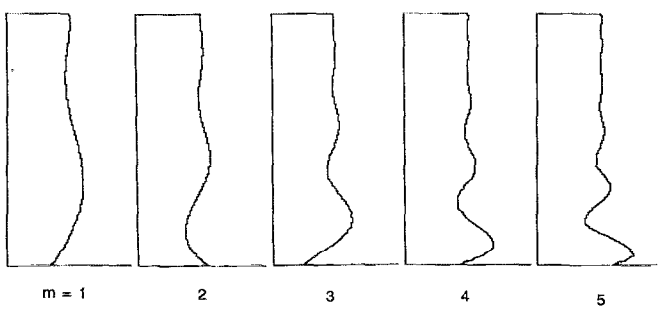

FIG. 4. Theoretical oscillation wave forms for various periodic modes. The $m=5$ and $m=2$ modes correspond to the pictures shown in parts (a) and (b) of Fig. 1.

The fact that laser fields are electromagnetic rather than acoustic is not really a fundamental distinction between these two types of oscillator. In fact there are also many acoustic masers having a variety of amplification mechanisms. An early example of an acoustic feedback oscillator is the humming telephone, which has been known for more than a century.[9] In the humming telephone there is an acoustic feedback path between the receiver (loudspeaker) and the transmitter (amplifying microphone), and the resulting system supports a wide variety of acoustic oscillation modes. The still older fluttering fountains discussed here may now be regarded as members in good standing of this same general feedback oscillator class.

ACKNOWLEDGMENTS

This work was supported in part by the National Science Foundation under Grant No. ECS-9014481. The author acknowledges valuable discussions with members of the Department of Physics at the University of Otago in Dunedin, New Zealand, and the assistance of M. W. Petrie and M. Singleton of the City Consultants of the Dunedin City Council. The author also acknowledges valuable discussions with E. Bodegom and M. Schumann of the Department of Physics at Portland State University, where an experimental fluttering fountain has recently been constructed.

[1] E. Loomis, Am. J. Sci. Arts **45**, 363 (1843).
[2] See, for example, G. L. Bragadin, A. Farina, M. Mancini, and R. Pompoli, in Proceedings of the 1988 International Conference on Noise Control Engineering (Inter-Noise 88), Avignon, France, 30 August–2 September 1988, pp. 931–934.
[3] L. W. Casperson, J. Sound Vib. **162**, 251 (1993).
[4] H. Helmholtz, Monatsberichte der königlich preussischen Akademie der Wissenschaften zu Berlin, 215 (1868) [translated in H. Helmholtz, London, Edinburgh, and Dublin, Philos. Mag. J. Sci. Ser. 4 **36**, 337 (1868)].
[5] M. Abramowitz and I. A. Stegun, Eds., *Handbook of Mathematical Functions* (U.S. GPO, Washington, DC, 1970), Eq. 19.1.2, p. 686.
[6] In Ref. 5, Eqs. 19.8.1 and 19.8.2, p. 689.
[7] H. I. Schwartz, Journal of the Hydraulics Division, Proceedings of the American Society of Civil Engineers, 1964, Vol. HY6, pp. 129–143.
[8] E. Naudascher, Journal of the Hydraulics Division, Proceedings of the American Society of Civil Engineers, 1965, Vol. HY3, pp. 389–392.
[9] L. W. Casperson, Opt. Quantum Electron. **23**, 995 (1991).